geosciences

MDPI

Article

Suitability of Boulder Marl and Marsh Clay as Sealing Substrates for Landfill Capping Systems—A Practical Comparison

Steffen Beck-Broichsitter [1,*], Horst H. Gerke [1] and Rainer Horn [2]

[1] Research Area 1 "Landscape Functioning", Working Group "Hydropedology", Leibniz-Centre for Agricultural Landscape Research (ZALF), Eberswalder Straße 84, 15374 Müncheberg, Germany; hgerke@zalf.de

[2] Institute of Plant Nutrition and Soil Science, Christian Albrechts University Kiel, Christian-Albrechts-Platz 4, 24118 Kiel, Germany; rhorn@soils.uni-kiel.de

* Correspondence: steffen.beck-broichsitter@zalf.de; Tel.: +49-33-432412

Received: 1 August 2018; Accepted: 17 September 2018; Published: 20 September 2018

Abstract: The effects of compaction on soil shrinkage behavior need to be considered for engineering long-term durable mineral liners of landfill capping systems. For this purpose, a new three-dimensional laser scanning device was coupled with a mathematical-empirical model to simultaneously determine the shrinkage behavior of a boulder marl (bm) and a marsh clay (mc). Therefore, both materials were precompacted in 200 soil cores (100 cm^3) on the basis of the Proctor test results with five different degrees of compaction (bm1-bm5; mc1-mc5). Thus, the shrinkage behavior, intensity, and tendency were determined during a standardized drying experiment. The volume shrinkage index was used to describe the pore size dependent shrinkage tendency and was classified as high to very high (11.3–17.7%) for the marsh clay and medium (5.3–9.2%) for the boulder marl. Additionally, only the boulder marl (bm2), compacted up to 88% of Proctor density, could be installed as landfill bottom liner in drier locations if the local matric potentials did not exceed the previously highest observed drying range (i.e. values below −300 hPa), to avoid crack formation and generation.

Keywords: landfill capping systems; mineral liner; shrinkage intensity and tendency

1. Introduction

Currently, landfills still represent the major option for global waste disposal in most areas of the world [1]. In Germany, the qualitative criteria of landfills are legally fixed [2]; they define the technical standards for engineered barriers [3].

The major aim of a landfill capping system is to restrain gas migration (e.g., carbon dioxide and methane), to minimize leachate generation in order to protect groundwater (precipitation contaminated with heavy metals or polycyclic hydrocarbons) by (a) high water storage capacity for the recultivated layer and (b) low hydraulic conductivity and negligible small shrinkage-crack formation potential for top and bottom liners [4,5]. Therefore, the plant-available water capacity and saturated hydraulic conductivity are considered essential properties of mineral sealing substrates (i.e., boulder marl and clay) according to a past paper [2]. These substrates are often used as landfill liners in combination with geosynthetics and geotextiles to ensure long-term hydraulic stability of the landfill capping systems [5,6].

They can also substitute geosynthetics and geotextiles, and enable the sustainable use of locally available resources. The materials selected must be suitable, and must have appropriate water content, before being installed [7]. The primary function of the bottom liner is not guaranteed if the actual, critical matric potentials within the mineral substrates are more negative than the pre-shrinkage

strength [8]. Thus, water and solutes can bypass through the newly formed shrinkage cracks in the mineral liners [9].

This case study presents laboratory measurements regarding the shrinkage behavior of boulder marl and marsh clay. The objective is the application of a new three-dimensional measurement device to better understand shrinkage-crack formation during drying cycles as a function of the matric potential coupled with a mathematical-empirical model.

The authors hypothesized that (a) the degree of compaction and corresponding water content strongly affects the shrinkage-induced volume change of both tested materials and (b) that the marsh clay is a more appropriate liner material than the boulder marl due to its soil hydraulic characteristics with respect to the statutory requirements for landfill liner.

Therefore, the shrinkage behavior of the marsh clay and boulder marl was analyzed in detail using the concept of critical matric potentials on the basis of the soil water retention characteristics, respectively.

2. Materials and Methods

2.1. Standard Proctor Compaction Tests

The boulder marl is derived from a pit located in the young moraine landscape (Rastorf: lat. 54°16′ N, long. 10°19′ E) and the clay is from decalcified marshland (Barlt: lat. 54°28′ N, long. 9°18′ E) in the state of Schleswig-Holstein in Northern Germany. Disturbed boulder marl and clay samples were used for four standard Proctor compaction tests (American Society for Testing and Materials D-698), respectively, and the degree of Proctor density D_{Pr} was calculated as follows [10],

$$D_{Pr} = \frac{\rho_t}{\rho_{Pr}} \quad (1)$$

where ρ_t denotes the dry bulk density (g cm^{-3}) and ρ_{Pr} is the proctor density (g cm^{-3}).

The clay and boulder marl samples were compacted to estimate the optimum water content (w_{opt}) and the maximum dry density (ρ_{topt}) for a Proctor compaction curve. Based on these results, homogenized marsh clay and boulder marl samples were moistened and compacted according to two different stages at the dry side (bm1, bm2, mc1, mc2) and wet side (bm4, bm5, mc4, mc5) of the moisture optimum (bm3, mc3), respectively. In total, 20 soil cores (diameter: 5.5 cm, height: 4 cm) per Proctor stage and the materials were prepared with a standard method by a load frame through a stamp (diameter: 5.5 cm) with a static load of 50 kN (Instron, Norwood, Mass, USA) for each selected stage of the Proctor curve (mc1-5, bm1-5).

2.2. Laboratory Analysis

Disturbed soil material was used to measure the organic carbon content at 1200 °C; soil texture was analyzed by the combined sieve (>63 µm) and pipette method, the soil pH value required preparation of a 0.01 M $CaCl_2$ solution (1:2 soil/suspension) (n = 40 for each undisturbed soil core); the particle density was determined by the pycnometer method and the dry bulk density (ρ_t) by the core method [11]. The saturated hydraulic conductivity (Ks) by the falling head method [12] with 10 undisturbed soil cores of clay and boulder marl, for each Proctor stage, respectively. The total porosity was calculated from the ratio between the dry bulk density and the particle density (bm: 2.63–2.64 g/cm^3, c: 2.67–2.68 g/cm^3). The water retention parameters were measured from undisturbed soil cores (n = 10 per Proctor stage) by a combined pressure plate (saturated, −30, −60, −150, −300, −500, and −1000 hPa) and −15,000 hPa ceramic vacuum outflow method, as well as being oven-dried for 16 h at 105 °C, respectively [11]. Simultaneous, the soil volume change at the different drying stages was estimated with the laser triangulation method as detailed described in Section 2.3.

The total porosity (TP) was calculated as ratio of dry bulk density and particle density (2.65 g/cm^3); air capacity (AC); and the plant available water capacity (AWC) are of major interest due to the statutory requirements for landfill capping systems and were calculated as follows:

$$AC = \theta_s - \theta_{FC} \quad (2)$$

$$AWC = \theta_{FC} - \theta_{WP} \quad (3)$$

where θ_s is the saturated water content (cm^3/cm^3), h is pressure head (hPa), and the subscripted symbols FC (field capacity) and WP (wilting point) indicate the water content at −60 hPa and −15,000 hPa, respectively.

2.3. Shrinkage Behavior and Volume Shrinkage Index

There are several noninvasive methods to evaluate the shrinkage behavior of soil cores including the manual combination of using a caliper and 2D photography to predict the shrinkage crack volume [13]. By contrast, the Soil-LT 100 (Umwelt-Geräte-Technik GmbH, Müncheberg, Germany) operates by the laser triangulation (LT) principle. The used line laser CMS 106 (Control Micro Systems, Orlando, FL, USA) illuminates a soil sample along a line on the soil sample cylinders surface. Its wavelength is around 0.66 µm, the laser class is designated as 1M. The laser line is projected from a point source and is aligned above the rotation center at the z-axis of the sample mount, depending on the region of interest, which defines the scan area (Figure 1). The laser line represents a cutting plane in x- and z-dimension of the instrument coordinate system, initially the retrieved coordinates of the 3D-scan featuring only x and z components. During the rotation, a charge coupled digital camera captures a predefined number of profiles while the camera is equipped with a band-pass filter to separate the laser signal (highlighted profile) in the captured image from the background [14,15]. Furthermore, shrinkage cracks can be very complex, but they can be indirectly recognized in regions of no data, because there is no surface to reflect the laser. For the standard volume calculation, the measurement point on the sample surface will be meshed to a surface and the crack will be closed, thus, Soil-LT software version 2.0 (Umwelt-Geräte-Technik GmbH, Müncheberg, Germany) features a tool to semi-automate the defining of crack areas. Additionally, the resulting soil volume relies on the calibration that provides a zero-level height [14,15].

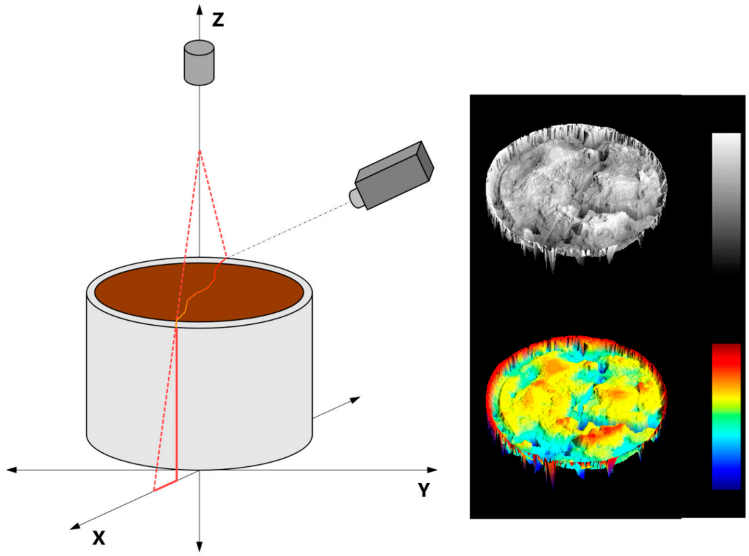

Figure 1. Soil-LT scanning operation with an undisturbed soil core (100 cm^3) rotating along the x-z plane (mm) while a coupled device camera (CCD) and a CMS 106 line laser (Control Micro Systems, Orlando, FL) detect and record the soil core surface (sample left) to create a 3D structure (samples right) using a software package (Umwelt-Geräte-Technik GmbH, Müncheberg, Germany).

The relation between the void ratio (e) and the moisture ratio (ϑ) defines the shrinkage curve according to a past paper [16],

$$e = \frac{V_f}{V_s} \tag{4}$$

$$\vartheta = \frac{V_w}{V_s} \tag{5}$$

where Vw, Vf, and Vs are the volumes of water, pores, and soils (cm^3/cm^3), respectively.

Considering the wide range of shrinkage models [17,18], the model of a past paper [16] was chosen due to its high validation standard for a wide range of soils as mentioned in several studies [19,20], even for compacted soils. Therefore, the modified van Genuchten equation (1980) was applied to adjust the shrinkage curve [16],

$$e(\vartheta) = \left\{ \begin{array}{ccc} e_r & & \vartheta = 0_s \\ & e_r + \frac{e_s - e_r}{\left[1+(\chi\vartheta)^{-p}\right]^q} \quad 0 \le \vartheta \le \vartheta_s; n > 0 & \\ e_s & & \vartheta = \vartheta_s \end{array} \right\} \tag{6}$$

where χ, p, and q are dimensionless fitting parameters, e_s and e_r are the saturated and residual void ratios that can be estimated by measurements. Additionally, the model of a past paper [16] fulfills the following boundary conditions:

$$\vartheta \to 0; \frac{\vartheta}{e_s - \theta} \to 0; e \to e_s \tag{7}$$

$$\vartheta \to \vartheta_s; \frac{\vartheta}{e_s - \vartheta} \to {}_o{}_o\infty; e \to e_s \tag{8}$$

The four phases of a typical shrinkage curve, known as (a) structural shrinkage, (b) proportional shrinkage, (c) residual shrinkage, and (d) zero shrinkage were determined mathematically using Equation (6) [16,21]. The sigmoidal shrinkage curve usually has two extreme curvatures at the wet side (ϑ_{shw} and e_{shw}) and at the dry side (ϑ_{shd} and e_{shd}) following the definition of a previous paper [16]. The maximum of the curve at the wet side (ϑ_{shw} and e_{shw}) is determined as the transition point between the structural and the proportional shrinkage phase, as determined previously [21,22]. In this study, we called this transition point the critical matric potential value (ψ_{mcrit}) for the boulder marl and marsh clay in the mineral sealing liner [23].

The volume shrinkage index (VSI) for the pore size dependent shrinkage tendency was defined as follows [15], wCP (wide coarse pores, >50 µm, 0 to −60 hPa), nCP (narrow coarse pores, 50–10 µm, −60 to −300 hPa), medium pores (MP, 10–2 µm, −300 to −15,000 hPa), and fine pores (<2 µm, <−15,000 hPa). The textural porosity is defined as pore space between the primary particles or micropores, while the structural porosity is characterized as the pore space between aggregates and contains macropores (i.e., biopores and shrinkage cracks) as previously described [24],

$$VSI_i = \frac{\Delta V_{ti}}{\Delta V_{pi}} - 1 \tag{9}$$

where ΔV_t is the soil volume in relation to the drained water-filled pore volume (ΔV_p) and i corresponds to the pore size (coarse, medium, and fine pores) of the respective drying stage.

The tendency of shrinkage (VSI) can be ranked into four classes: low (<5%), moderate (5–10%), high (10–15%), and very high (>15%) according to a past paper [25]. The coefficient of activity (I_A) describes the swelling and shrinkage potential of soil material and can be determined as follows [25].

$$I_A = \frac{I_P}{\%\ clay} \tag{10}$$

Where I_P is the plasticity index due to the Atterberg limit test [26]. The coefficient of activity (I_A) can be ranked into three classes: $I_A < 0.75$ (inactive material), $0.75 < I_A < 1.25$ (normal active material), and >1.25 (active material). The clay mineralogy was determined with X-ray diffraction analysis (D8 Discover, Bruker AXS, Billerica, MA, USA).

2.4. Statistical Analysis

The mean values and standard deviations for each sampling depth were calculated. An analysis of variance (ANOVA) with $p < 0.05$ verified the effect of pore size distribution and degree of compaction on the pore functions and the volume shrinkage index (VSI). Differences of means were assessed by Tukey's HSD test ($p < 0.05$) as described previously [27]. The correlation coefficient (r^2) is an index of goodness of fit.

3. Results

3.1. Basic Soil Characteristics

The sandy loam (SL) textured boulder marl (bm) and a silty clay loam (SiL) textured marsh clay (c) are characterized by a clay content of 11% and 26%, a moderately acidic (pH 5.6) or slightly alkaline character (pH 7.6) with an organic carbon content of 0.25% and 0.05%, respectively (Table 1).

Table 1. Basic soil characteristics of the landfill capping system for marsh clay (mc) and boulder marl (bm), n = 4 repeated measurements for organic carbon (OC), pH value, texture, and particle density (ρs). The symbol ± corresponds to the standard deviation. SL = CL = * [28].

Material	OC [%]	pH [$CaCl_2$]	Sand [%]	Silt [%]	Clay [%]	ρ_t [g/cm^3]	Texture *
bm	0.05 ± 0.02	7.6 ± 0.3	68 ± 1	21 ± 2	11 ± 2	2.65 ± 0.2	SL
mc	0.25 ± 0.03	5.6 ± 0.2	18 ± 1	56 ± 2	26 ± 3	2.67 ± 0.3	CL

The boulder marl and the marsh clay are characterized by coefficients of activity of 0.18 ± 0.1 and 0.69 ± 0.4, respectively that corresponds to an inactive material (Table 2). Thus, the ability for swelling and shrinkage is restricted for both materials, especially for the kaolinite dominated marsh clay.

The boulder marl mainly consists of quartz (85–88%) and calcite (3–4%), smectite (2–11%), and vermiculite (1–4%). In contrast, the marsh clay mainly consists of quartz (21–25%), kaolinite (34–36%), illite (22–24%), and montmorillonite (14–16%).

Table 2. Coefficients of activity (I_A) and clay mineralogy of marsh clay (mc) and boulder marl (bm) with n = 3 per material. The symbol ± corresponds to the standard deviation.

Material	I_A [-]	Quarz [%]	Calcite [%]	Kaolinite [%]	Smectite [%]	Vermiculite [%]	Illite [%]	Mont-Morillonite [%]
bm	0.18 ± 0.1	85–88	3–4	-	3–11	3–4	-	-
mc	0.69 ± 0.4	21–25	0.5–1	34–36	-	-	22–24	14–16

The marsh clay has very small ρt values (1.08 g/cm^3 to 1.11 g/cm^3) and was compacted to a Proctor density of D_{Pr} 80% to 82%. The intermediate to firm ρt values between 1.66 g/cm^3 and 1.94 g/cm^3 of the boulder marl were comparatively higher with D_{Pr} values between 78% and 92% (Figure 2).

The Ks values of the marsh clay varied between 1.2×10^{-7} m/s and 7.4×10^{-7} m/s and of the boulder marl between 3.8×10^{-7} m/s and 1.2×10^{-7} m/s (Table 3). The TP values of the marsh clay decreased with increasing moisture content while the Proctor optimum (bm3) showed the lowest TP value for the boulder marl. Additionally, the sealing layer thickness should vary between 1.2 m (mc3) and 7.4 m (mc1) for the marsh clay and between 3.8 m (bm3) and 12.0 m (bm5) for the boulder marl,

they reach the same permeation rate, like a 0.5 m thick layer with a Ks value of 5×10^{-9} m/s, while the Ks values of both tested materials were 2- or 3-orders in magnitude higher.

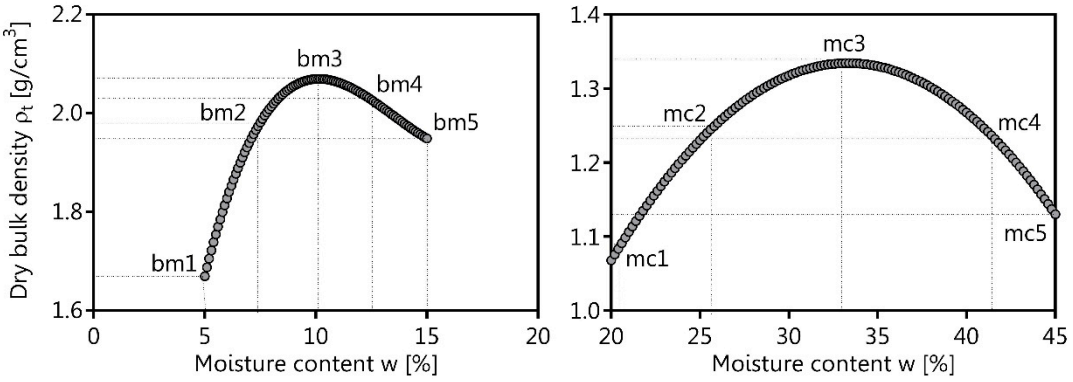

Figure 2. Moisture content (w, %), Proctor density (Pr) and the degree of proctor density (D_{Pr}, %) of five different Proctor stages of the boulder marl (bm1-5) and the clay (mc1-mc5), respectively (n = 4).

Table 3. Soil physical properties of the investigated clay (mc1-mc5) and boulder marl (bm1-bm5) considering the shrinkage-dependent volume changes for the average total porosity (TP), air capacity (AC), the plant available water capacity (AWC), moisture content (w), proctor density (ρ_{Pr}), and degree of proctor density (D_{Pr}), n = 10 soil cores per Proctor stage. The symbol ± corresponds to the standard deviation.

ProctorStage	TP [cm^3/cm^3]	AC [cm^3/cm^3]	AWC [cm^3/cm^3]	ρ_t [g/cm^3]	W [%]	ρ_{Pr} [g/cm^3]	D_{Pr} [%]	Ks [m/s]
mc1	0.657	0.115	0.256	1.10	20	1.09	80	$7.4 \pm 2.3 \times 10^{-7}$
mc2	0.648	0.096	0.253	1.09	25	1.25	81	$3.2 \pm 1.6 \times 10^{-7}$
mc3	0.637	0.582	0.244	1.11	33	1.35	82	$1.2 \pm 0.8 \times 10^{-7}$
mc4	0.604	0.043	0.255	1.09	41	1.23	80	$3.8 \pm 1.4 \times 10^{-7}$
mc5	0.592	0.033	0.271	1.08	45	1.10	80	$6.8 \pm 3.2 \times 10^{-7}$
bm1	0.426	0.051	0.081	1.66	5.0	1.67	78	$1.6 \pm 1.3 \times 10^{-6}$
bm2	0.401	0.054	0.076	1.85	7.5	1.98	88	$1.8 \pm 1.2 \times 10^{-6}$
bm3	0.302	0.026	0.059	1.94	10.1	2.07	92	$1.2 \pm 0.5 \times 10^{-6}$
bm4	0.329	0.049	0.069	1.85	12.5	2.03	87	$7.8 \pm 2.1 \times 10^{-7}$
bm5	0.352	0.056	0.067	1.78	15.0	1.95	84	$3.8 \pm 1.6 \times 10^{-7}$

The air capacity (AC) of the marsh clays vary between 0.033 cm^3/cm^3 (mc5) and 0.115 cm^3/cm^3 (mc1) and the AC values of the boulder marl ranged from 0.026 cm^3/cm^3 (bm3) to 0.056 cm^3/cm^3 (bm5). Furthermore, marsh clay was characterized by plant available water capacities (AWC) of 0.244 cm^3/cm^3 (mc3) and 0.271 cm^3/cm^3 (mc5) and the boulder marl by AWC values between 0.033 cm^3/cm^3 and 0.081 cm^3/cm^3. Thus, the TP and AWC values of the marsh clay are significantly higher than the TP and AWC values of the boulder marl (Table 3).

Additionally, the study results show that the required recultivation layer thickness to achieve 0.14 cm^3/cm^3 per meter varies between 1.73 m (bm1) and 2.38 m (bm3) for the boulder marl, and between 0.55 m (mc1) and 0.58 m (mc3) for the marsh clay.

3.2. Shrinkage Behavior and Volume Shrinkage Index

In total, two different stages at the dry side (mc1, mc2, bm1, bm2) and wet side (mc4, mc5, bm4, bm5) of the moisture optimum (mc3, bm3) were chosen for further investigations. The void and moisture ratios ($e_s = \vartheta_s$) of the marsh clay varied between 1.78 cm^3/cm^3 and 1.91 cm^3/cm^3 in the following order, mc1 > mc2 > mc3 < mc4 < mc5, so, the moisture optimum (mc3) is described by the lowest void ratio and moisture ratio (Table 4). For the boulder marl, the void and moisture ratios

($e_s = \vartheta_s$) varied between 0.42 cm^3/cm^3 and 0.70 cm^3/cm^3 in the following order, bm1 > bm2 > bm3 < bm4 < bm5, so, the moisture optimum (bm3) is described by the lowest void and moisture ratio.

Table 4. Parameters derived from shrinkage curves of the Proctor stages of marsh clay (mc1-mc5) and boulder marl (bm1-bm5) according to a previous model [16]: saturated void and moisture ratio (e_s and ϑ_s), the transition point between the structural and the proportional shrinkage phase (e_{shw} and ϑ_{shw}), the change of void ratio (e) and moisture ratio (ϑ) during the structural shrinkage phase (e_s-e_{shw} and ϑ_s-ϑ_{shw}), and the proportional shrinkage phase (e_{shw}-e_{shd} and ϑ_{shw}-ϑ_{shd}). The symbol ± corresponds to the standard deviation.

Proctor Stage	χ [-]	p [-]	q [-]	r^2 [-]		e_{shw}, ϑ_{shw} [cm^3/cm^3]	e_s-e_{shw}, ϑ_s-ϑ_{shw} [cm^3/cm^3]	e_{shw}-e_{shd}, ϑ_{shw}-ϑ_{shd} [cm^3/cm^3]
mc1	0.539	61.85	0.014	0.99	ϑ	1.85	0.001 ± 0.001	1.75 ± 0.01
					e	1.75	0.015 ± 0.001	1.15 ± 0.02
mc2	0.525	72.54	0.014	0.98	ϑ	1.79	0.001 ± 0.001	1.68 ± 0.03
					e	1.77	0.02 ± 0.001	1.34 ± 0.01
mc3	0.716	11.62	0.120	0.99	ϑ	1.39	0.02 ± 0.003	1.29 ± 0.02
					e	1.66	0.001 ± 0.001	1.30 ± 0.02
mc4	0.563	87.47	0.014	0.99	ϑ	1.77	0 ± 0.001	1.68 ± 0.01
					e	1.77	0 ± 0.001	1.33 ± 0.02
mc5	0.504	275.1	0.002	0.99	ϑ	1.91	0 ± 0.001	1.71 ± 0.02
					e	1.91	0 ± 0.001	1.42 ± 0.03
bm1	1.356	236.5	0.003	0.98	ϑ	0.70	0.001 ± 0.001	0.60 ± 0.06
					e	0.692	0.001 ± 0.001	0.09 ± 0.003
bm2	10.2	6.269	1129	0.98	ϑ	0.35	0.15 ± 0.02	0.24 ± 0.04
					e	0.48	0.02 ± 0.001	0.07 ± 0.01
bm3	2.40	0.014	4.116	0.97	ϑ	0.417	0.001 ± 0.001	0.32 ± 0.7
					e	0.42	0.001 ± 0.001	0.06 ± 0.002
bm4	2.001	132.5	0.014	0.96	ϑ	0.50	0 ± 0.001	0.40 ± 0.05
					e	0.510	0 ± 0.001	0.06 ± 0.002
bm5	1.81	64.19	0.014	0.99	ϑ	0.522	0.023 ± 0.001	0.44 ± 0.06
					e	0.555	0 ± 0.0001	0.06 ± 0.003

The proportional shrinkage phase was the major shrinkage phase of the Proctor stages starting between 0 hPa and −30 hPa under continuous drying, with the exception of mc3 that reached the proportional shrinkage phase between −30 and −60 hPa (e_{shw}: 1.666 cm^3/cm^3 and ϑ_{shw}: 1.386 cm^3/cm^3). Nearly identical results were indicated for the boulder marl, with the exception of bm2 that reached the proportional shrinkage phase at about −300 hPa (e_{shw}: 0.472 cm^3/cm^3 and ϑshw: 0.342 cm^3/cm^3). For the boulder marl, the volume loss during the proportional shrinkage phase (e_{shw}-e_{shd} and ϑ_{shw}-ϑ_{shd}) was indicated by changes in the void ratios between 0.06 cm^3/cm^3 and 0.09 cm^3/cm^3, and changes in the moisture ratios between 0.24 cm^3/cm^3 and 0.60 cm^3/cm^3 (Figures 3 and 4). On the other hand, the proportional shrinkage phase of the clay was characterized by changes in the moisture ratios between 1.29 cm^3/cm^3 and 1.75 cm^3/cm^3 and void ratios between 1.15 cm^3/cm^3 and 1.42 cm^3/cm^3.

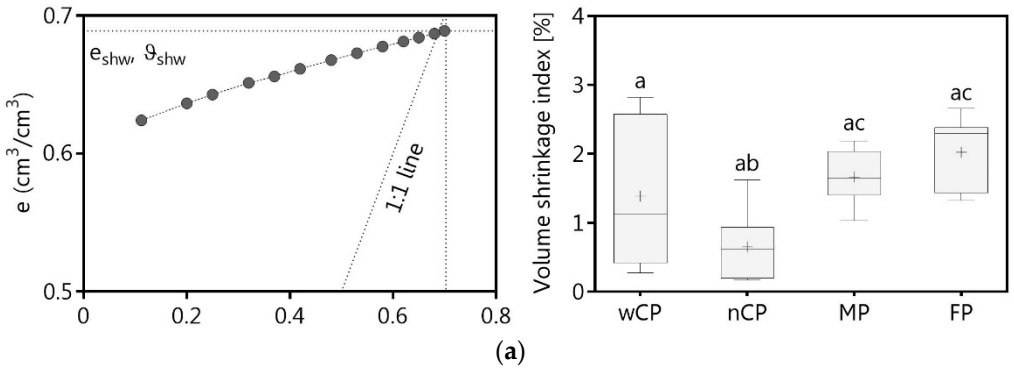

(**a**)

Figure 3. *Cont.*

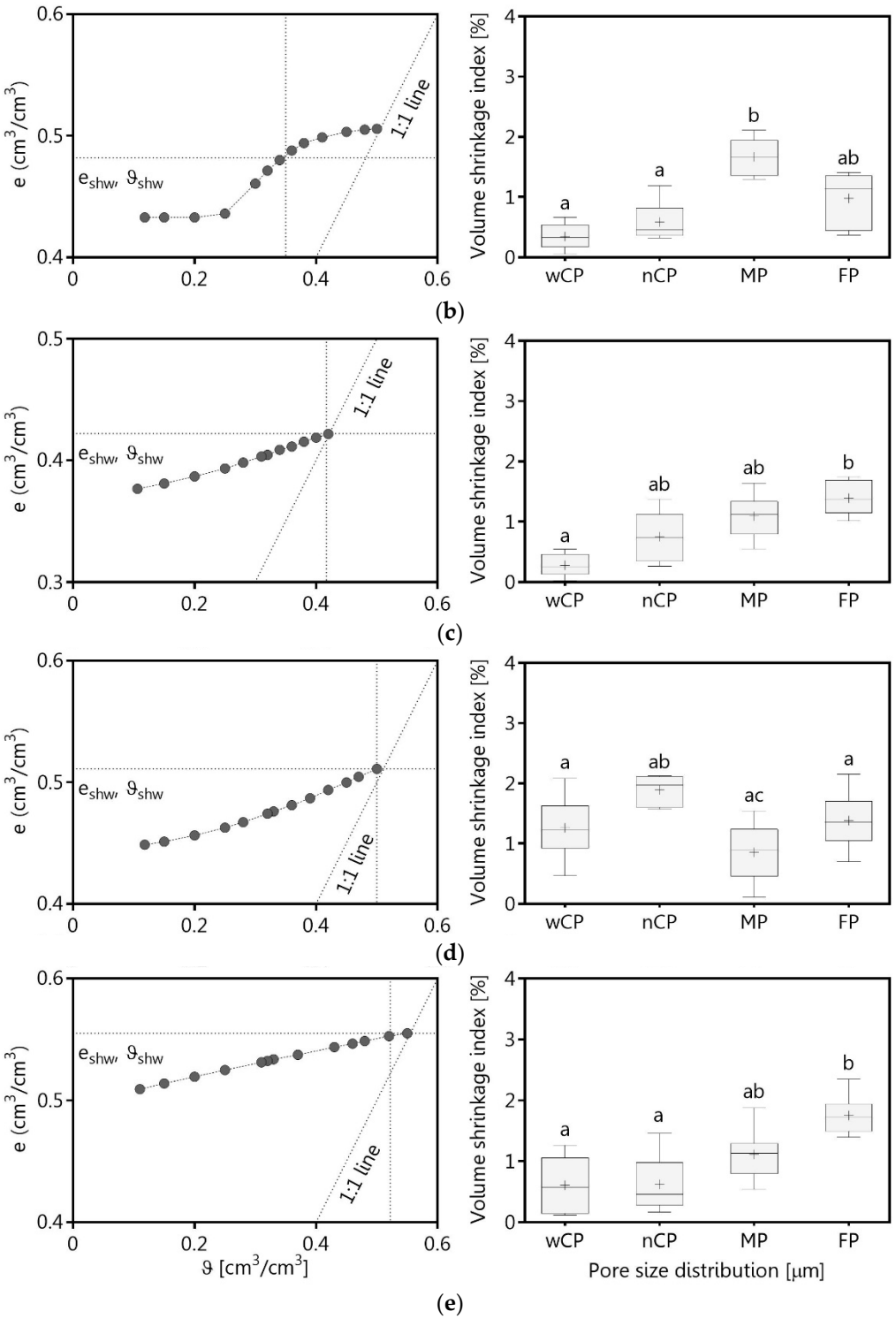

Figure 3. Shrinkage curves and volume shrinkage index of the wide coarse (wCP), narrow coarse pores (nCP), medium (MP), and fine pores (FP) of the five different Proctor stages: (**a**) bm1, (**b**) bm2, (**c**) bm3, (**d**) bm4, (**e**) bm5. Different letters indicate statistically significant differences ($p < 0.05$) of the volume shrinkage index in comparison to the pore size. The transition point between the structural and the proportional shrinkage phase is marked with dashed lines (e_{shw} and ϑ_{shw}).

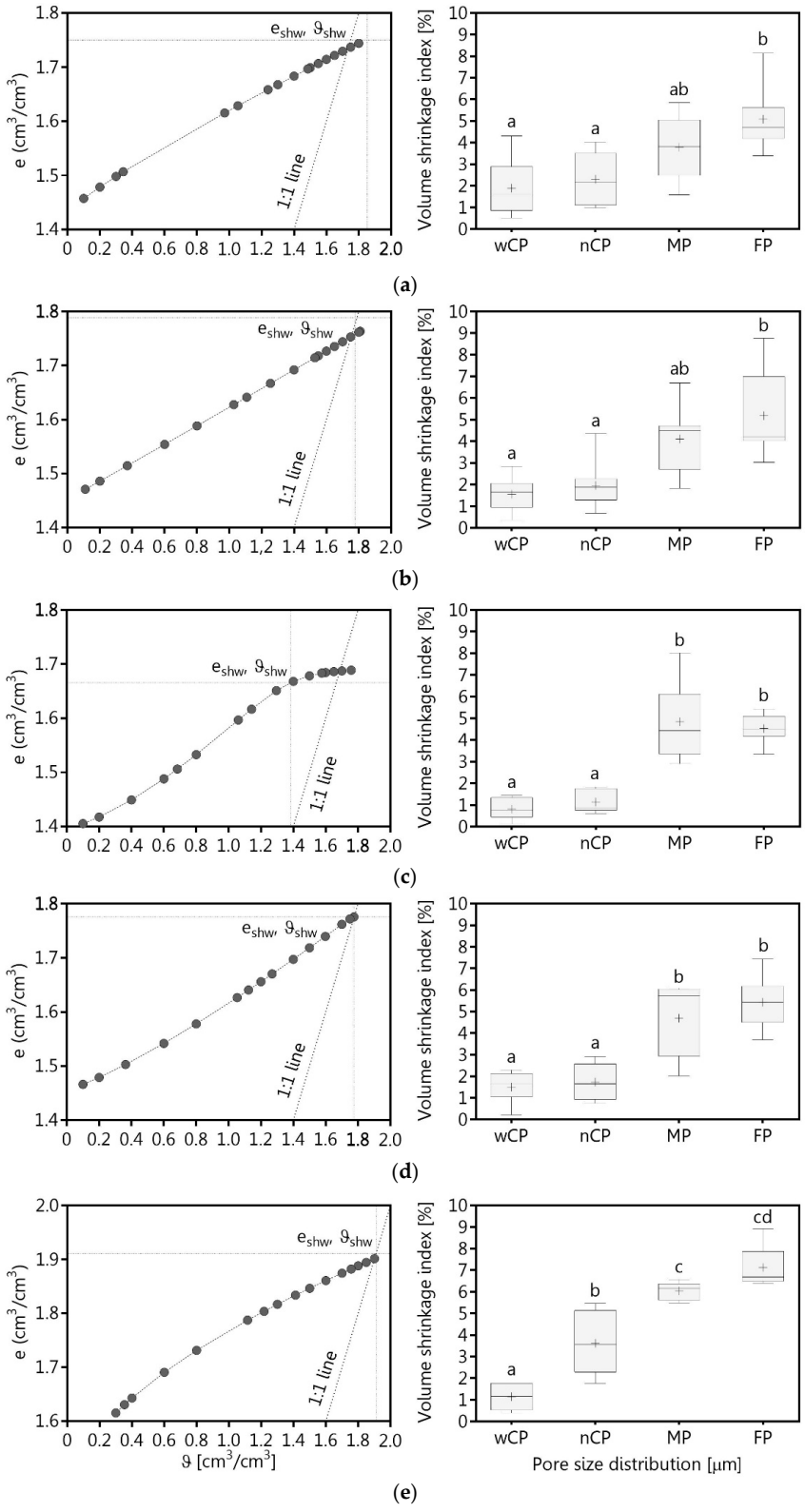

Figure 4. Shrinkage curves and volume shrinkage index of the wide coarse (wCP), narrow coarse pores (nCP), medium (MP), and fine pores (FP) of the five different Proctor stages: (**a**): mc1, (**b**): mc2, (**c**): mc3, (**d**): mc4, (**e**): mc5. Different letters indicate statistically significant differences ($p < 0.05$) of the volume shrinkage index in comparison to the pore size. The transition point between the structural and the proportional shrinkage phase is marked with dashed lines (e_{shw} and ϑ_{shw}).

The structural shrinkage phase (mc1-mc5) was less pronounced with changes in the void and moisture ratios (e_s-e_{shw} and ϑ_s-ϑ_{shw}) of between 0 cm^3/cm^3 and 0.02 cm^3/cm^3 and a residual shrinkage phase that could not be clearly determined (Figures 3 and 4). Nearly identical results were indicated for the boulder marl, whereby the only exception, bm2, showed a volume loss during the structural shrinkage phase described by changes of void ratio of 0.02 cm^3/cm^3 and moisture ratio of 0.15 cm^3/cm^3.

The exceedance of the pre-shrinkage stress (ψ_{mcrit}) also resulted in a more distinctive volume change (e_{shw}-e_{shd}) during the proportional shrinkage phase than in the structural shrinkage phase. The shrinkage model simulated the results of void ratio (e) and moisture ratio (ϑ) very well with coefficient relations of $r^2 \geq 0.96$ (Table 4).

The volume shrinkage index (VSI) of the clay and the boulder marl, summed up from the wide and narrow coarse pores as well as medium and fine pores, could be classified as high to very high for the marsh clay with 12.8% for mc3 and 17.9% for c5, and as medium shrinkage tendency for the boulder marl with 5.4% for bm2 and 9.3% for bm1 (Figures 3 and 4). The volume shrinkage indices of the marsh clay and the boulder marl were positively correlated with the fine pore content (r^2: 0.38, boulder marl r^2: 0.40), and the void ratios decreased with increasing dry bulk density (r^2: 0.60, r^2: 0.85), respectively (Figure 5).

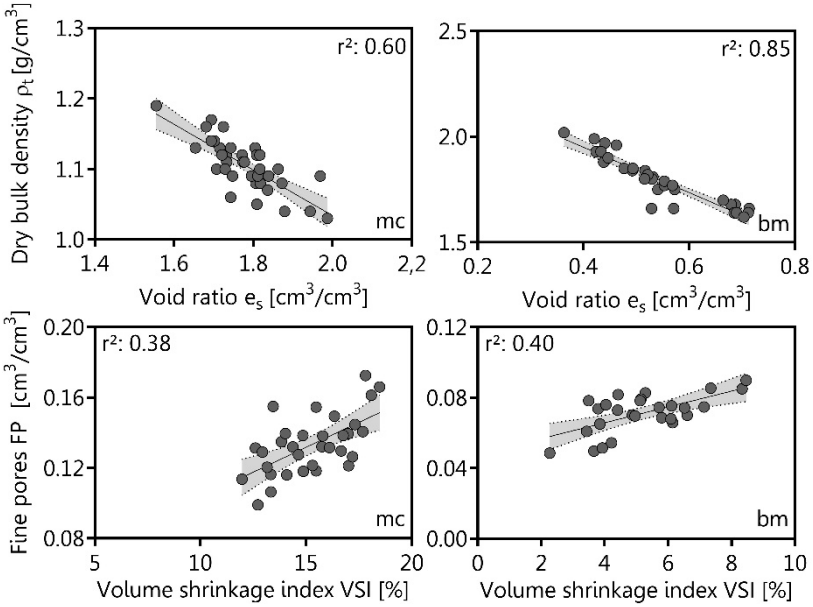

Figure 5. Volume shrinkage indices as a function of the fine pores (FP) and the void ratio, as a function of the dry bulk density (ρt), of marsh clay (mc, n = 40) and boulder marl (bm, n = 40) with regard to the regression function, respectively. The r^2 indicates the coefficient of determination. The dashed lines indicate the confidence limits for a confidence level of 95%.

4. Discussion

4.1. Statutory Requirements of the German Landfill Directive

The German Landfill Directive, which was enacted in 2009, includes the essential statutory requirements to achieve the securing of closed landfills: (a) available water capacity of the recultivation, or rather, topsoil layer of at minimum 0.14 cm^3/cm^3 per meter, (b) Ks values of at least 5×10^{-9} m/s equal to 0.5 m thickness and a hydraulic gradient of I = 0.3 m, and (c) AC values of at minimum 0.08 cm^3/cm^3.

Therefore, the marsh clay would be a more appropriate recultivation material to reach the statutory requirements excluding the shrinkage crack formation properties of the clay [29]. The comparatively lower AWC values of the boulder marl can be explained, and are related to the smaller number of

nCP and MP as mentioned previously [30], thus, an increasing AWC could be realized with compost addition [31] or with increasing compaction, as previously [32] pointed out. As result of this, a higher transpiration rate and water storage capacity could reduce the amount of infiltrating water, as described previously [33]. Considering the Ks values, neither the boulder marl nor the marsh clay are suitable materials for the sealing layer according to the authors of a past paper [2].

The natural permeability may be reduced by additional compaction [34], but it is well-known that a reduced number of coarse pores accompany soil compaction, along with smaller Ks values, especially in the top and bottom liner, when compared with uncompacted, natural soils [33]. Thus, even if these values cannot be reached, the consideration of shrinkage processes and anthropogenic anisotropic flow properties (Ks horizontal > vertical) of the liner can help make the top and bottom liners impermeable for the long-term. The Ks values could be lowered by the addition of three-layer clayey minerals (i.e., montmorillonite), but due to the high-water absorption capacity of these minerals, the shrinkage-crack initiation moisture content could potentially increase [35,36].

Additionally, the required threshold value for the air capacity of ≥ 0.08 cm^3/cm^3 could only be reached by the marsh clay (mc1, mc2) on the dry side of the Proctor curve, so, the installation of marsh clay and boulder marl as a top liner cannot guarantee optimal plant growth, thus resulting in restricted transpiration potential [3].

4.2. Shrinkage Behavior of Marsh Clay and Boulder Marl

The long-term hydraulic stability of landfill liners is of major interest for the environmental police and thus, the statutory requirements, and therefore this study, are focused on the soil physical properties of mineral liners including (a) shrinkage behavior, (b) shrinkage intensity, and (c) shrinkage tendency as cumulative factor. In this context, several studies [29,37] mentioned that the shrinkage behavior of natural soils strongly depends on the soil texture, soil structure, and compaction, while the mechanical and hydraulic pre-stress are mostly ignored. In contrast, the authors of a previous paper [38] stated that (a) shrinkage behavior is a result of the rearrangement of soil particles and pores by mechanical and hydraulic stresses resulting in soil compaction with different effects on the changes of pore diameter and continuity and (b) that the intensity depends primarily on the existence of swelling clay. Thus, the clay content and type of clay are only one part that should be added by organic carbon content as confirmed previously [9].

In general, soil shrinkage is mainly due to textural pores rather than to structural pores [24]. In this case, artificial soil compaction (including Proctor test experiments) may reduce the volume of structural pores considerably, while most of the textural pores remain unaffected, according to previous investigations [13,18,39]. So, the higher number of medium and fine pores in the marsh clay could also be a reason for the more pronounced proportional shrinkage [19,40], inversely proportional to the fitting parameter χ, as previously mentioned [20]. This coincides with the effect of a complete initial homogenization prior to the laboratory experiments. It is to be expected that those moistened soil samples undergo a more intense cracking, down to very negative matric potential values compared to those of structured or rather aggregated soils, as shown previously [38].

The explanation of the shrinkage intensity requires some knowledge about the clay mineral fraction of the liner material. In general, the shrinkage intensity is more pronounced the higher the amount of three-layer clayey minerals (i.e., smectite/vermiculite/montmorillonite), as compared to the two-layer and also to the four-layer minerals they have a better shrinkage and swelling capacity [41,42]. Thus, the more pronounced volume shrinkage tendency of the marsh clay could be attributed to the presence of illite and montmorillonite [41] while the percentage of non-swelling and shrinking kaolinite does not alter the shrink swell patterns.

The new phenomenon in this context is the fact that the application of hydraulic or mechanical stresses alters the soil pore system differently. Therefore, the marsh clay, with its lower ρt values, reacts more strongly to than the boulder marl due to the more pronounced volume shrinkage tendency, which agrees with past investigations [29,30]. During the Proctor test, the amount of removed water

for complete shrinkage increases, and consequently, the volume shrinkage tendency also increases [23]. As a result, this increases the volume shrinkage index on the wet side of the Proctor curve (c4-c5, bm4-bm5), especially for the marsh clay, which agrees with past findings [5]. The combination of compaction (dynamic) and added water affects the matric potential status resulting in complete water saturated systems under the influence of cyclic loading and unloading. Under those conditions, the pore water pressure of the added water continuously pushes soil particles apart while decreasing the friction between them [11], thus, the arrangement of particles has a pronounced effect on the shrinkage-induced volume change [23,37], and therefore, the shrinkage intensity as a cumulative effect.

4.3. Suitability of Marsh Clay and Boulder Marl as Mineral Liner

Summing up all influential factors, the suitability of mineral liner is superficially limited by shrinkage-crack formation, frost impact, or root penetration in conjunction with increasing Ks values of approximately three orders of magnitude [43], resulting in higher infiltration and leachate rates by a factor of 3 to 4 [44] due to preferential macropore flow, especially during intensive precipitation events [24].

On that note, the proposed concept of critical matric potentials is very useful to describe suitability of both materials as mineral liner. The boulder marl, in form of the bm2 with a ψ_{mcrit} value of −300 hPa, would be an effective bottom liner, if (a) it is installed on the dry side of the Proctor curve near the Proctor optimum, (b) the Ks values closely correspond to the statutory requirements, and (c) no desiccation effects more negative than the mentioned one can be expected in the bottom liner, even in drier periods. On the other side, the marsh clay should not be used for top liners and despite its low permeability [4], the shrinkage-crack potential, even for less negative matric potentials, is very pronounced and endangers the hydraulic stability of landfill capping systems. The use as bottom liner, even though the c3 with a ψ_{mcrit} value of −30 to −60 hPa, would be more effective for more humid locations, where no desiccation effects more negative than −60 hPa can be expected in the bottom liner.

The results suggest that several conflicts of interest exist (i.e., shrinkage intensity versus Ks values) and both materials are not usable as bottom liner with an exclusive purchase on the soil physical properties, respectively. Thus, the boulder marl is a more useful top liner material with its less pronounced shrinkage potential and can also be installed as bottom liner in combination with clayey substrates or geosynthetics and geotextiles, decreasing its comparatively higher permeability due to subsequent compaction during installation [33]. Alternatively, temporary capping systems mostly consist of semipermeable mineral liner to slowly shout down the so called 'bioreactor' and therefore, the investigated boulder marl with its permeability characteristics should be the material of choice as mentioned by [31].

Therefore, the pretreatment of the material, such as repeated desiccation and/or in combination with previous compaction, can even in humid climates, affect the long-term impermeability and safety of such landfill capping systems. This is true, because exceeding the previously highest drying or compaction range inevitably results in the next crack formation and generation [45]. Thus, if the matric potential can be more negative than the critical matric potential (pre-shrinkage stress) due to higher hydraulic stress of the menisci forces in the micropores [13,38], then proportional shrinkage can irreversible cause further shrinkage-crack formation [39].

This circumstance limits the suitability of the marsh clay, especially for drier locations, where the matric potentials in the bottom liner regularly exceed the critical matric potential range, as mentioned before. If this advice is ignored, documented studies, i.e., at the "Georgswerder landfill" (Hamburg,) have shown irreversible shrinkage-cracks in mineral liners [44] after exceeding the pre-shrinkage stress, thus, the presence of shrinkage cracks can be recognized as a key factor for mineral liner degradation [35,43].

This fact depends on the thickness of the top liner, the climate conditions, and the initial moisture content during the installation, even with a more pronounced swelling potential, but if cracked, the healing potential is very limited, even if the proportional shrinkage phase is reached [43]. This finding

is summed up in a past paper [11], such healing would require dynamic processes like shearing or kneading, which are not possible in the bottom liner [33], even for both tested materials that were indexed as inactive with a restricted swelling and shrinkage ability. Additionally, roots can restrict crack formation due to the larger shear strength of rooted systems, but they also can hinder the self-healing of cracks during the wetting process [43].

5. Conclusions

The results allow us to conclude that the soil water retention characteristics and shrinkage behavior, tendency, and intensity of both tested materials are affected by (a) the degree of compaction and (b) the corresponding water content. Considering the statutory requirements for landfill liner, neither the boulder marl, nor the marsh clay completely fulfill the required soil hydraulic characteristics for a long-term functional mineral landfill liner.

The results also show that the volume change during the drying phase is less pronounced for the soil material that was installed on the dry side of the Proctor curve below the optimum for Proctor compaction, thus, the initial moisture content during the installation of mineral liners is of major interest. Additionally, processes such as wetting and drying, root growth and penetration, and freeze-thaw cycles could potentially reduce the hydraulic stability for both tested materials (e.g., increase the permeability and the pore continuity) of the top and bottom liner even in a short time after installation of the liners in a landfill capping system.

Thus, it should be kept in mind that the hydraulic stability or rather the shrinkage-crack formation resistance of top or bottom liners consisting of marsh clay or boulder marl could be ensured by (a) a high pre-shrinkage stress ($\psi_{mfield} > \psi_{mcrit}$), (b) a water content as low as possible during the installation phase ($\theta_{field} > \theta_{installation}$), (c) shallow-rooting plants, and (d) a less pronounced shrinkage intensity and shrinkage tendency.

Author Contributions: S.B.-B., H.H.G., and R.H. conceived the presented idea. S.B.-B. contributed the methodology, software, validation, visualization, and the formal analysis of the presented data. R.H. and H.H.G. supervised the findings of this study including conceptualization, supervision, reviewing and editing, draft preparation, and project administration.

Funding: This research was founded by the Innovation Foundation of the federal state of Schleswig-Holstein and the ZMD Rastorf GmbH, Germany.

Acknowledgments: The Innovation Foundation of Schleswig-Holstein financially supported this study and I thank the reviewers for the helpful comments.

Conflicts of Interest: The funders had no role in the design of the study; in the collection, analyses, or interpretation of data; in the writing of the manuscript, or in the decision to publish the results

References

1. Hoornweg, D.; Bhada-Tata, P. *What a Waste: A Global Review of Solid Waste Management*; Urban Development Series, Knowledge Papers (15); The World Bank: Washington, DC, USA, 2012.
2. The German Federal Government. *Degree on Landfills (Ordinance to Simplify the Landfill Law)—Germany, in the Form of the Resolution of the Federal Cabinet*; The German Federal Government: Berlin, Germany, 2009.
3. Hauser, V.L. *Evapotranspiration Covers for Landfills and Waste Sites*; CRC Press, Taylor & Francis: Boca Raton, FL, USA, 2008.
4. Arnold, S.; Schneider, A.; Doley, D.; Baumgartl, T. The limited impact of vegetation on the water balance of mine waste cover systems in semiarid Australia. *Ecohydrology* **2014**, *8*, 355–367. [CrossRef]
5. Widomski, M.K.; Stępniewski, W.; Horn, R.; Bieganowski, A.; Gazda, L.; Franus, M.; Pawlowska, M. Shrink-swell potential, hydraulic conductivity and geotechnical properties of clay materials for landfill liner construction. *Int. Agrophys.* **2015**, *29*, 365–375. [CrossRef]
6. Laner, D.; Crest, M.; Schraff, H.; Morris, J.W.F.; Barlaz, M.A. A review of approaches for the long-term management of municipal solid waste landfills. *Waste Manag.* **2012**, *32*, 498–512. [CrossRef] [PubMed]
7. Horn, R.; Stępniewski, W. Modification of mineral liner to improve its long-term stability. *Int. Agrophys.* **2004**, *18*, 317–323.

8. Witt, K.J.; Zeh, R.M. Crack due Desiccation in Cover Lining Systems Phenomena and Design Strategy. In Proceedings of the Hydro-Physico-Mechanics of Landfills, Grenoble, France, 21–22 March 2005; Grenoble University: Grenoble, France, 2005.
9. Costa, S.; Kodikara, J.; Shannon, B. Salient factors controlling desiccation cracking of clay in laboratory experiments. *Géotechnique* **2013**, *63*, 18–29. [CrossRef]
10. Proctor, R.R. Design and Construction of Rolled Earth Dams. Master's Thesis, University of Louisville, Louisville, France, 1933.
11. Hartge, K.H.; Horn, R. *Essential Soil Physics—An Introduction to Soil Processes, Structure, and Mechanics*; Horton, R., Horn, R., Bachmann, J., Peth, S., Eds.; Schweizerbart Science Publishers: Stuttgart, Germany, 2016.
12. Hartge, K.H. Ein Haubenpermeameter zum schnellen Durchmessen zahlreicher Stechzylinderproben. Z. Kulturtech. *Flurbereinigung* **1966**, *7*, 155–163.
13. Peng, X.; Horn, R.; Peth, S.; Smucker, A. Quantification of soil shrinkage in 2D by digital image processing of soil surface. *Soil Till Res.* **2006**, *91*, 173–180. [CrossRef]
14. Seyfarth, M.; Holldorf, J.; Pagenkemper, S.K. Investigation of shrinkage induced changes in soil volume with laser scanning technique and automated soil volume determination—A new approach/method to analyze pore rigidity limits. *Soil Till Res.* **2012**, *125*, 105–108. [CrossRef]
15. Umwelt-Geräte-Technik GmbH. *Soil-LT 100—Device for Combined Volume, Weight and Water Tension Measurement. Operating Instructions*; Umwelt-Geräte-Technik GmbH: Müncheberg, Germany, 2015.
16. Peng, X.; Horn, R. Modelling soil shrinkage curve across a wide range of soil types. *Soil Sci. Soc. Am. J.* **2005**, *69*, 584–592. [CrossRef]
17. Chertkov, V.Y.; Ravina, I.; Zadoenko, V. An approach for estimating the shrinkage geometry factor at a moisture content. *Soil Sci. Soc. Am. J.* **2004**, *68*, 1807–1817. [CrossRef]
18. Braudeau, E.; Frangi, J.P.; Mothar, R.H. Characterizing non-rigid dual porosity structured soil medium using its characteristic SC. *Soil Sci. Soc. Am. J.* **2004**, *68*, 359–370. [CrossRef]
19. Gebhardt, S.; Fleige, H.; Horn, R. Anisotropic shrinkage of mineral and organic soils and its impact on soil hydraulic properties. *Soil Till Res.* **2012**, *125*, 96–104. [CrossRef]
20. Peng, X.; Horn, R. Identifying six types of soil shrinkage curves from a large set of experimental data. *Soil Sci. Soc. Am. J.* **2013**, *77*, 372–381. [CrossRef]
21. Peng, X.; Horn, R. Anisotropic shrinkage and swelling of some organic and inorganic soils. *Eur. J. Soil Sci.* **2007**, *58*, 98–107. [CrossRef]
22. Groenevelt, P.H.; Grant, C.D. Curvature of shrinkage lines in relation to the consistency and structure of Norwegian clay soil. *Geoderma* **2002**, *106*, 235–245. [CrossRef]
23. Horn, R.; Baumgartl, T. Dynamic properties of soils. In *Soil Physics Companion*; Warrick, A.W., Ed.; CRC Press LLC: Boca Raton, FL, USA, 2002; pp. 17–48.
24. Alaoui, A.; Lipiec, J.; Gerke, H.H. A review of the changes in the soil pore system due to soil deformation: A hydrodynamic perspective. *Soil Till Res.* **2011**, *115–116*, 1–15. [CrossRef]
25. Skempton, A.W. The Colloidal "Activity" of Clays. In Proceedings of the Third International Conference on Soil Mechanics, Zürich, Swiss, 16–27 August 1953; pp. 57–61.
26. Terzaghi, K.; Peck, R.B. *Soil Mechanics in Engineering Practise*; John Wiley: New York, NY, USA, 1967.
27. R Development Core Team. *R: A Language and Environment for Statistical Computing*; R Foundation for Statistical Computing: Vienna, Austria, 2008.
28. FAO. *Guidelines for Soil Description*; FAO-ISRIC Press: Rome, Italy, 2006.
29. Huang, C.; Shao, M.; Tan, W. Soil shrinkage and hydrostructural characteristics of three swelling soils in Shaanxi, China. *J. Soils Sediments* **2011**, *11*, 474–481. [CrossRef]
30. Schäffer, B.; Schulin, R.; Boivin, P. Changes in shrinkage of restored soil caused by compaction beneath heavy agricultural machinery. *Eur. J. Soil Sci.* **2008**, *59*, 771–783. [CrossRef]
31. Beck-Broichsitter, S.; Fleige, H.; Horn, R. Waste capping systems processes and consequences for the longterm impermeability. In *Soils within Cities*; Levin, M., Kim, H.J., Morel, J.L., Burghardt, W., Charzynski, P., Shaw, R.K., Eds.; Catena Soil Sciences: Stuttgart, Germany, 2018; pp. 148–152.
32. Anlauf, R.; Rehrmann, P. Effect of compaction on soil hydraulic parameters of vegetative landfill covers. *Geomaterials* **2012**, *2*, 29–36. [CrossRef]

33. Stępniewski, W.; Widomski, M.K.; Horn, R. Hydraulic conductivity and landfill construction. In *Developments in Hydraulic Conductivity Research, Rijeka, Croatia, 2011*; Dikinya, O., Ed.; Intech: Rijeka, Croatia, 2011; pp. 249–270.
34. Zhang, S.L.; Grip, H.; Lovdahl, L. Effect of soil compaction on hydraulic properties of two loess soils in China. *Soil Till Res.* **2006**, *90*, 117–125. [CrossRef]
35. Albright, W.; Benson, C.; Gee, G.; Abichou, T.; Tyler, S.; Rock, S. Field Performance of a compacted clay candfill final cover at a humid site. *J. Geotech. Geoenviron. Engr.* **2006**, *132*, 1393–1403. [CrossRef]
36. Priyankara, N.H.; Abeyrathne, W.K.A.P.; Alagiyawanna, A.M.W.; Kawamoto, K. Investigation of suitability of expansive soil to use as clay liners. In Proceedings of the 14th International Waste Management and Landfill Symposium, Sardinia, Italy, 30 September–4 October 2013; pp. 55–62.
37. Habib, A.S. Effect of compaction characteristics on shrinkage of expansive clay. *Res. J. Eng. Appl. Sci.* **2013**, *2*, 439–445.
38. Horn, R.; Peng, X.; Fleige, H.; Dörner, J. Pore rigidy in structured soils—only a theoretical boundary condition for hydraulic properties. *J. Soil Sci. Plant Nutr.* **2014**, *60*, 3–14.
39. Oleszczuk, R.; Brandyk, T. The analysis of shrinkage-swelling behavior of peat-moorsh soil aggregates during drying-wetting cycles. *Agron. Res.* **2008**, *6*, 131–140.
40. Beck-Broichsitter, S.; Fleige, H.; Goebel, M.-O.; Dörner, J.; Bachmann, J.; Horn, R. Shrinkage potential and pore shrinkage capacity of differently developed volcanic ash soils under pastures in southern Chile. *J. Plant Nutr. Soil Sci.* **2016**, *179*, 799–808. [CrossRef]
41. Ajayi, A.; Horn, R. Comparing the potentials of clay and biochar in improving water retention and mechanical resilience of sandy soil. *Int. Agrophys.* **2016**, *30*, 391–399. [CrossRef]
42. Markgraf, W.; Watts, C.W.; Whalley, W.R.; Hrkac, T.; Horn, R. Influence of organic matter on rheological properties of soil. *Appl. Clay Sci.* **2012**, *64*, 25–33. [CrossRef]
43. Li, J.H.; Li, L.; Chen, R.; Li, D.Q. Cracking and vertical preferential flow through landfill clay liners. *Eng. Geol.* **2016**, *206*, 33–41. [CrossRef]
44. Melchior, S.; Sokollek, V.; Berger, K.; Vielhaber, B.; Steinert, B. Results from 18 Years of in-situ performance testing of landfill cover systems in Germany. *J. Environ. Eng.-Am. Soc. Civ. Eng.* **2010**, *136*, 815–823. [CrossRef]
45. Gebhardt, S.; Fleige, H.; Horn, R. Shrinkage processes of a drained riparian peatland with subsidence morphology. *J. Soils Sediments* **2010**, *10*, 484–493. [CrossRef]